Desalination and Water Treatment
www.deswater.com

1944-3994/1944-3986 © 2012 Desalination Publications. All rights reserved
doi: 10/5004/dwt.2012.2743

Taylor & Francis
Taylor & Francis Group

40 (2012) 129–136
February

Adsorption of Astrazon Blue FGRL onto sepiolite from aqueous solutions

Atakan Ongen*, H. Kurtulus Ozcan, Emine Elmaslar Ozbas, Nilgün Balkaya

Department of Environmental Engineering, Istanbul University, 34320, Avcilar, Istanbul, Turkey
Tel. +90 212 4737070; Fax: +90 212 4737180; email: aongen@istanbul.edu.tr

Received 21 February 2011; Accepted 7 September 2011

ABSTRACT

In this study, adsorption of Astrazon Blue FGRL on sepiolite (meerschaum) from aqueous solution was investigated using different parameters like initial dye concentration, temperature, contact time and solution pH. The obtained results were then compared for all the parameters. At the end of batch adsorption studies, the equilibrium time, optimum pH and temperature were 90 min, 7 pH and 293 K, respectively. Adsorption isotherm of Astrazon Blue FGRL on sepiolite (meerschaum) was determined and correlated with common isotherm equations such as Langmuir and Freundlich models. The Freundlich model ($r^2 > 0.98$) appeared to fit the isotherm data better than the Langmuir model ($r^2 < 0.92$). The kinetic data for sepiolite (meerschaum) supported the pseudo-second-order model ($r^2 > 0.99$), through the first order kinetic model did not adequately fit the experiment values ($r^2 < 0.99$). SEM, XRD and FT-IR spectrum analyses were carried out. The obtained results showed that Sepiolite (meerschaum) can be an alternative low-cost adsorbent for removing dye from wastewater.

Keywords: Sepiolite; Adsorption; Isotherms; Kinetic models; Astrazon Blue FGRL

1. Introduction

Organic dyes are used in many industries such as food, paper, carpet, rubber, plastics, cosmetics, and textile in order to color their products [1–4]. They can be classified as anionic (direct, acid, and reactive dyes), cationic (basic dyes) and non-ionic (disperse dyes) [1]. The discharge of colored wastewater from these industries into natural streams causes many significant problems like increasing the toxicity and COD (chemical oxygen demand) of the effluent and reducing the light penetration, which has a derogatory effect on photosynthetic phenomenon. In addition, stringent color consent standards are enforced by regulatory bodies to reduce the quantity of color in effluent and receiving water courses [5].

Dyeing effluents are very difficult to treat due to their resistance to biodegradability, stability to light, heat and oxidizing agents [6–8]. In general, the treatment of dye-containing effluents is undertaken by adsorption, oxidation–ozonation, biological processes, coagulation–flocculation and membrane processes [9].

The adsorption process provides an attractive alternative treatment, especially if the adsorbent is inexpensive and readily available because of its low cost, simplicity of design, high efficiency, ease of operation, biodegradability, and ability to entrap dyes in a concentrated form [1,6,10]. Activated carbon is the most popular adsorbent for the adsorption process since it has a high surface area that increases the adsorption capacity, but due to its difficult and expensive regeneration, an alternative low-cost and easily available adsorbent is still needed. [1,5,11]. Natural clays for dye removal

---

*Corresponding author.

from wastewater such as sepiolite [12–15], kaolinite [16], montmorillonite [17], smectite [18] and bentonite [19,20] are therefore considered as alternative low-cost adsorbents [10].

Sepiolite (meerschaum) is a clay mineral with fibrous habit and ideal formula $Mg_8Si_{12}O_{30}(OH)_4(OH_2)_4 \cdot nH_2O$ ($n \le 8$) [21–25], commonly used as adsorbent, filler, catalyst or catalyst support [26–28]. Its structure consists of discontinuous z-elongated octahedral (O) strips and waving tetrahedral (T) sheets, in which the apical oxygen atoms alternately bond to the upper or lower O strip. This arrangement causes the structure to be crossed by microtunnels along z (dimensions: 1.06 × 0.37 nm), filled by weakly bound zeolitic H_2O and possibly exchangeable cations. Tightly bound structural OH_2 completes the coordination of Mg-ions located at the borders of the O strips, protruding in the tunnels. Sepiolite (meerschaum) has a broad variety of useful properties and applications, due to its characteristic microporosity and high surface area. It is mostly used for sorptive applications, since it can retain up to 250% of its own weight in water located in the channels or bonded to the surface. Sepiolite (meerschaum) is also widely used as a decolorizing agent [5,25,29].

This mineral is widely used to remove undesired components from household and industrial wastewaters and also in various industrial manufacturing processes, including the removal of organic compounds [30], heavy metals [31], ammonium and phosphate, anionic dyes (reactive blue 221 and acid blue 62), phenol and lignin [5].

In this study, the removal of Astrazon Blue FGRL from aqueous solutions using the low-cost material sepiolite (meerschaum) as the adsorbent by means of batch adsorption techniques was investigated. The common Langmuir and Freundlich equations were used to fit the equilibrium isotherm. The dynamic behavior of the adsorption was examined in terms of the effects of initial dye concentration, temperature and pH. The adsorption rates were determined quantitatively and simulated with the pseudo-first-order and pseudo-second-order kinetic models.

2. Experimental

2.1. Materials

A commercial textile dye – Astrazon Blue FGRL (AB FGRL) – was obtained from Dystar, Turkey and used without further purification. This dye consists of two main components, C.I. Basic Blue 159 and C.I. Basic Blue 3, their ratio benig 5:1 (w/w), respectively. The structures of two dye components are displayed in Fig. 1.

This basic dye is not regarded as acutely toxic, but it can have various harmful effects [32,33]. This dye is mainly used as acrylic dyeing in the industry.

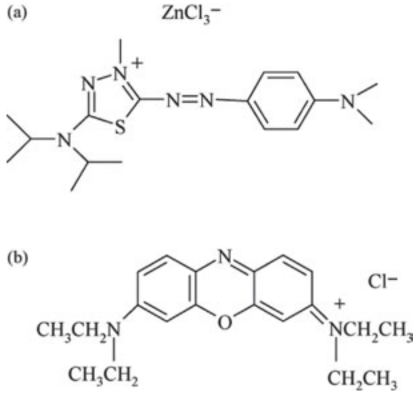

Fig. 1. Chemical structures of C.I. Basic Blue 159 (a) and C:I. Basic Blue 3 (b).

Sepiolite (meerschaum) used in this study was provided from Eskisehir Region, Turkey. It was crushed, ground, sieved through a 0.5–2 mm sieve, treated with distilled water to remove soluble impurities and dried at 105°C for 2 h prior to use.

The infrared spectrum of samples were carried out with Digilab, Exalibur-FTS 3000 MX model (USA) in the range of 400–4000 cm^{-1}. In order to prepare the sample pellets, the samples were diluted with IR grade Merck KBr (samples/KBr: 1/200 (w/w)).

For SEM analysis, JEOL/JSM-6335F model scanning electron microscope with 1000× and 50,000× magnification was used. The specific surface area (BET) of sepiolite (meerschaum) sample was derived from N_2 adsorption isotherms measured at liquid nitrogen temperature using a Quantachrome Instruments Nova 4000E instrument.

2.2. Adsorption experiments

Adsorption experiments were conducted in a thermostatic shaker bath at 283, 293 and 313 K at constant initial concentration (100 mg l^{-1}). The initial concentrations of dye solutions were in the range of 25, 50, 100, 150 and 200 mg l^{-1} and experiments were performed at 293 K. The contact time, initial dye concentration, initial pH, and temperature were selected as experimental parameters. The pH of the solution was adjusted with NaOH or HNO_3 solution by using a pH-meter (Hanna Instruments pH213 pH meter) equipped with a combined electrode. At the end of the adsorption period, the solution was centrifuged for 10 min at 5000 rpm and the concentration of dye remaining in the supernatant determined with a 1.0 cm light path quartz cells using a spectrophotometer (PG Instruments T 60U UV/VIS) at λ_{max} of 599 nm. The amount of adsorbed dye was calculated from the concentrations in the solution both before and after the adsorption. The calibration curve was plotted from the dye solutions prepared in the concentrations of 10–300 mg l^{-1}. All experiments were repeated at least twice.

2.3. Adsorption kinetics

Several kinetic models are available to understand the behavior of the adsorbent and to examine the controlling mechanism of the adsorption process and test the experimental data. In the present investigation, the adsorption data were analyzed by using two kinetic models: the pseudo-first-order and pseudo-second-order. Conformity between the experimental data and the model-predicted values was expressed by means of the related correlation coefficients (r^2). A relatively high r^2 value indicates that the model successfully describes the kinetics of the dye adsorption. The pseudo-first-order model was presented by Lagergren [34].

A pseudo-first-order equation can be expressed in a linear form as:

$$\log(q_e - q) = \log\left(q_e\right) - (k_1/2.303)t \tag{1}$$

where q_e and q is the amounts of dye adsorbed (mg g^{-1}) on the adsorbents at equilibrium and at time t, respectively; and k_1 is the rate constant of adsorption (min^{-1}). Values of k_1 were calculated from the plots of log(q_e–q) versus t for different concentrations of the basic dye.

The sorption data was also analyzed in terms of pseudo-second-order mechanism described in Refs. [35,36].

The pseudo-second-order adsorption kinetic rate equation is expressed as:

$$\mathrm{d}\, q_t/\mathrm{d}\, t = k_2\left(q_e - q_t\right)^2 \tag{2}$$

where k_2 is the rate constant of pseudo-second-order adsorption (g mg^{-1} min). Integrating and applying the initial conditions, we have a linear form as:

$$t/q_t = \left[1/\left(k_2 q_e^{\,2}\right)\right] + \left(1/q_e\right)(t) \tag{3}$$

where q_e is the amount of dye adsorbed at equilibrium (mg g^{-1}). The second-order rate constants were used to calculate the initial sorption rate, $h = k_2 q_e^{\,2}$. In addition, k_2 and q_e values were calculated from the intercept and the slope of the linear plots of t/q_t versus t.

2.4. Adsorption isotherms

The adsorption isotherm indicates how the adsorbate molecules distribute between the liquid and solid phases when the adsorption process reaches an equilibrium state. The analysis of the isotherm data by fitting them to different isotherm models is an important step to find a suitable model for design purposes [1,37]. In adsorption isotherm study, Langmuir and Freundlich equations are generally used as adsorption isotherm equations. For the liquid–solid system, the Langmuir and Freundlich isotherm equations basically assume that sorption can occur at specific sites within the adsorbent, and no further adsorption can take place at sites occupied by dye molecules. Therefore, a saturation point is reached at equilibrium. No further adsorption can occur beyond this point. Thus, the saturation monolayer can be represented by the following expression [38]:

$$\left(C_e/q_e\right) = \left(1/q_m K\right) + \left(1/q_m\right) C_e \tag{4}$$

where q_m is the maximum amount of adsorption (mg g^{-1}); K is the affinity constant (l g^{-1}) and C_e is the solution concentration at equilibrium (mg l^{-1}). The Freundlich model assumes that the sorption takes place on heterogeneous surfaces and adsorption capacity depends on the concentration of dyes at equilibrium. The well-known logarithmic form of Freundlich model is given by the following equation [38]:

$$\ln q_e = \ln K_F + \left(1/n\right)\ln C_e \tag{5}$$

where K_F and n is the Freundlich constants related to adsorption capacity and adsorption intensity, respectively. So, the plot of lnq_e against lnC_e in Eq. (5) should give a linear relationship whereby $1/n$ and K_F can be determined from the slope and the intercept, respectively.

3. Results and discussion

3.1. SEM analysis

As stated in the literature, the fiber length and thickness of layered sepiolite as bundles of fiber can range between 100 Å and 5 mm and between 50 and 100 Å, respectively [39,40]. However, the length of fibers in sepiolite varies depending on the source of sepiolite. The maximum fiber length and maximum thickness of Eskişehir sepiolite, Turkey was determined approximately as 4–5 μm and 50–100 Å [41]. Scanning electron microscopy (SEM) micrographs of sepiolite (meerschaum) samples are shown in Fig. 2. SEM micrograph of the sepiolite showed that it has a fibrous structure that there is a good possibility for dye to be trapped and adsorbed into this structure.

In BET measurements, specific surface area of raw sepiolite (meerschaum) was determined as 377.916 m^2 g^{-1}.

3.2. FT-IR analysis

The FTIR spectrum of raw sepiolite (meerschaum) is given in Fig. 3 The spectrum of raw sepiolite (meerschaum) has the characteristic bands at 3691 cm^{-1} (stretching vibrations of hydroxyl groups attached to octahedral Mg ions located in the interior blocks), 3581 cm^{-1} (H–O–H stretching vibrations of water molecules

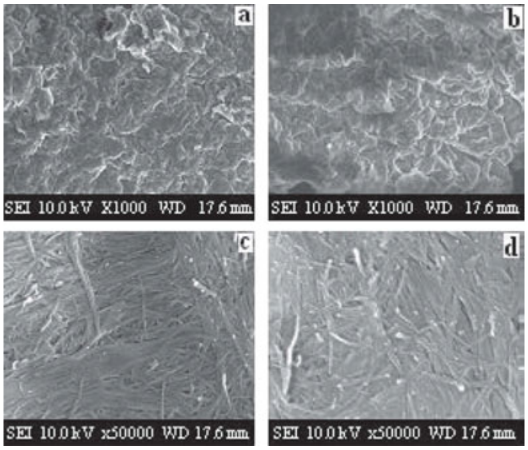

Fig. 2. SEM photographs of raw sepiolite (a, c), and AB FGRL adsorbed sepiolite sample (b, d).

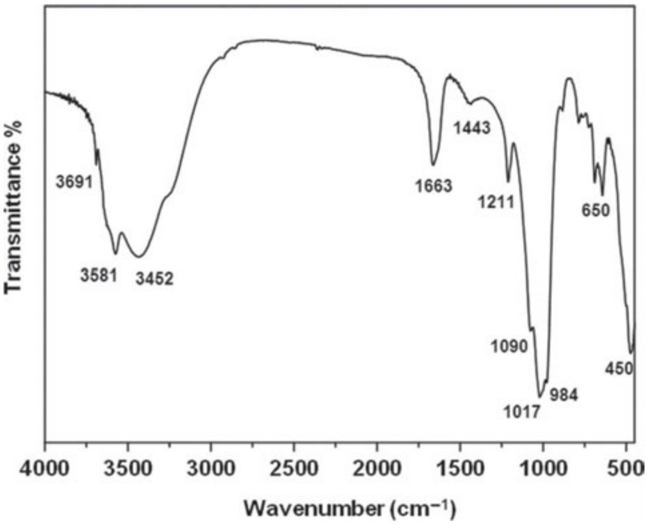

Fig. 3. The FTIR spectrum of raw sepiolite sample.

weakly hydrogen bonded to the Si–O surface), and 3452 cm^{-1} (water OH-stretch), 1,663 cm^{-1} (OH-bending). The broad band around 3000–4000 cm^{-1} is due to H–O–H vibrations of adsorbed water [5,42,43].

In addition, the spectrum of raw sepiolite (meerschaum) had also the characteristic lattice vibrations at 1211; 1090 and 984 cm^{-1} (the Si–O combination bands), 1017 cm^{-1} (the basal plane of the tetrahedral units exhibiting the Si–O–Si plane vibrations), 450 cm^{-1} (Si–O–Mg of the octahedral–tetrahedral linkage) and 650 cm^{-1} (Mg_3OH-bending vibration) [21,22,43,44]. Dolomite impurities resulted in 1443 cm^{-1} band [5,21,24,43].

The FTIR spectrums of both raw sepiolite (meerschaum) and AB FGRL adsorbed sepiolite (meerschaum) are given together in Fig. 4 to allow straight comparison. Chemical interaction may occur between the organic molecule (dye) and clay matrix. FTIR analyses of dye adsorbed on clay (sepiolite) confirmed this interaction.

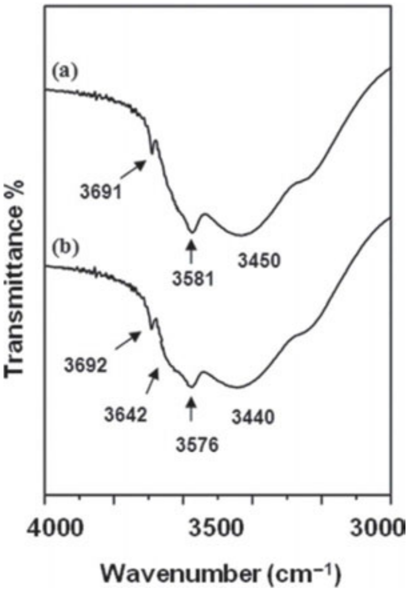

Fig. 4. The FTIR spectrum of raw sepiolite (a) and AB FGRL absorbed sepiolite (b).

In case of interactions between organic molecule (dye) and clay (sepiolite), adsorbed dye molecule may be coordinated to oxygen plane (Si–O–Si) through water molecules. In addition, water molecules may displace from coordination sphere by dye molecules and it may take place a direct linkage with exchangeable cation in the interlayer [17,27]. This situation is observed as a new shoulder or broad peak at 3642 cm^{-1} in the OH stretching region in FTIR spectrum. In addition, the broad OH stretching band was shifted from about 3450 to about 3440 cm^{-1}. Therefore, FTIR spectra of sepiolite and Astrazon Blue indicate and confirm interactions of the guest dye with hosting matrix structure [21].

3.3. *Effect of initial dye concentration*

The effect of initial dye concentrations on adsorption rate of sepiolite (meerschaum) is in the range from 25 to 200 mg l^{-1} (Fig. 5).

The influence of the initial concentration of AB FGRL in the solutions on the adsorption rate of sepiolite (meerschaum) was investigated at various concentrations and pH 7. As shown in Fig. 5, the adsorption capacity of the dye increased from 29 to 293 mg g^{-1} by increasing the initial dye concentration from 25 to 200 mg l^{-1}. This indicates the importance of initial dye concentration on the adsorption capacities of AB FGRL onto sepiolite (meerschaum).

3.4. *Effect of temperature*

Fig. 6 shows the effect of temperature and contact time on the adsorption process. The equilibrium adsorption capacity of AB FGRL onto sepiolite (meerschaum) is

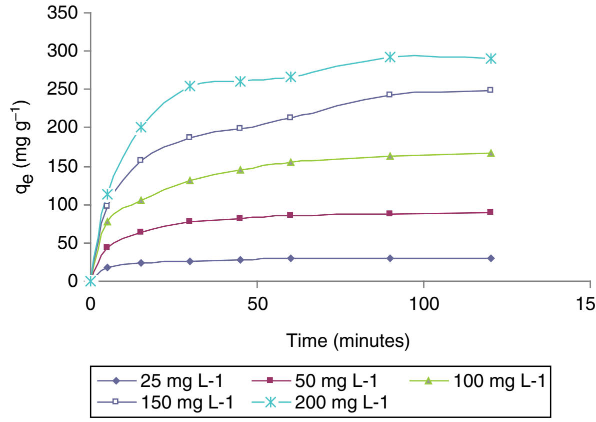

Fig. 5. Effect of initial dye concentration and contact time (0.1 g 200 ml^{-1} adsorbent, 293 K, pH = 7, 200 rpm).

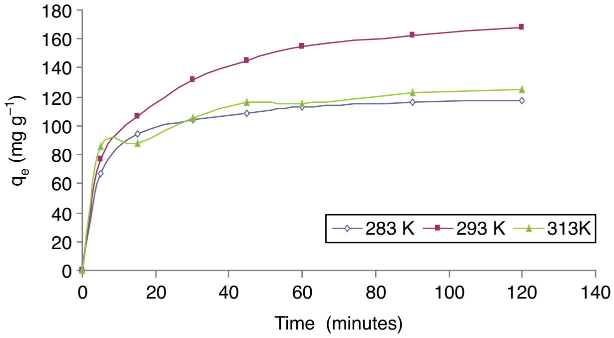

Fig. 6. Effect of temperature and contact time (0.1 g 200 ml^{-1} adsorbent, 100 mg l^{-1} initial dye concentration, pH = 7, 200 rpm).

also affected by temperature; this effect was investigated at 283, 293 and 313 K. As seen in Fig. 6, the optimum temperature is 293 K (the amount of adsorbed dye is 84 mg g^{-1}).

The equilibrium adsorption capacity of sepiolite (meerschaum) decreased from 84 to 61 mg g^{-1} at a concentration of 100 mg l^{-1} with temperature increasing from 283 to 313 K (Fig. 6). Accordingly, the adsorption of AB FGRL onto sepiolite (meerschaum) surface is favored at lower temperatures and controlled by an exothermic process. This is partly due to a weakening of the attractive forces [10,45,46] between AB FGRL and sepiolite (meerschaum).

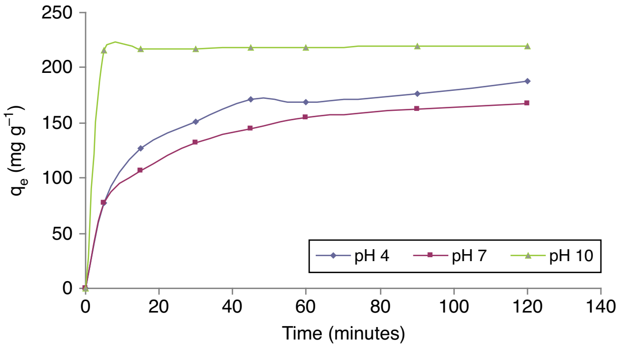

Fig. 7. Effect of pH and contact time (0.1 g 200 ml^{-1} adsorbent, 100 mg l^{-1} initial dye concentration, 293 K, 200 rpm).

3.5. Effect of pH

The pH of the solution affects the surface charge of the adsorbents as well as the degree of ionization of different pollutants. The hydrogen and hydroxyl ions are adsorbed quite strongly, and therefore the adsorption of other ions is affected by the pH of the solution. Change of pH affects the adsorptive process through dissociation of functional groups on the active sites of adsorbent surface. Consequently, this leads to a shift in reaction kinetics and equilibrium characteristics of adsorption process [47]. The adsorption of AB FGRL on sepiolite (meerschaum) was studied in a pH range of 4–10 at 293 K and for 120 min. Initial dye concentration was 100 mg l^{-1}. Fig. 7 shows the effect of pH on the removal rate of AB FGRL on sepiolite (meerschaum).

The removal of AB FGRL by sepiolite (meerschaum) was increased with pH rise until pH = 10. Alkan et al. found that sepiolite (meerschaum) had a isoelectrical point at pH 6.6 and exhibited positive zeta potential values at lower pH values (6.6) and negative zeta potential values at higher pH values [48]. In this case, sepiolite (meerschaum) has negative zeta potential above pH 6.6. Thus, it would be suitable to use higher pH values than isoelectrical point pH for the adsorption of cationic dyes. As the pH of the dye solutions becomes higher than the isoelectrical point pH, the association of dye cations with negatively charged sepiolite (meerschaum) surface can more easily take place as follows:

$$SO^{-} + Dye^{+} = SO^{-}Dye^{+} \tag{6}$$

According to Eq. (6), the adsorption rate of AB FGRL dyes on sepiolite (meerschaum) increases with alkaline pH values. Similarly, other studies reported higher removal rates of AB FGRL in the alkaline pH range [47–52].

3.6. Adsorption kinetics

In order to quantify the applicability of the pseudo-first-order and pseudo-second-order models, correlation coefficients (r^2) were calculated from the plots. The linearity of these plots indicates the applicability of both models. However, the correlation coefficients (r^2) showed that the experimental data fit the pseudo-second-order model ($r^2 \approx 0.998 - 0.999$) better than the pseudo-first-order model ($r^2 \approx 0.773-0.997$) (Figs. 8 and 9, Table 1). This was observed in the comparison of q_e values obtained from the pseudo-first-order plots with the experimental q_e values. The experimental q_e values and those obtained from the slopes of the pseudo-second-order plots showed a better agreement (Table 1).

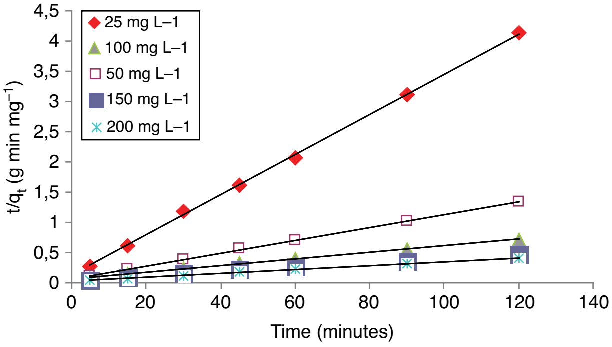

Fig. 8. Second-order kinetic equation for adsorption of AB FGRL (293 K, solid–liquid ratio: 0.1 g 200 ml^{-1}, pH 7, particle size: 0.1–2.5 mm).

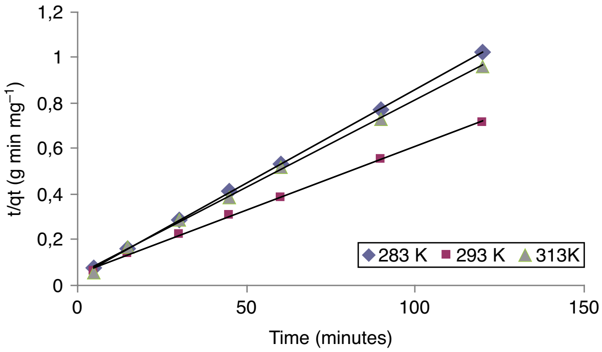

Fig. 9. Second-order kinetic equation for adsorption of AB FGRL (100 mg l^{-1}, solid–liquid: 0.1 g 200 ml^{-1}, pH = 7, particle size: 0.1–2.5 mm).

3.7. Isotherm studies

The Langmuir and Freundlich parameters for the adsorption of AB FGRL are listed in Table 2. Isoterm coefficients in Table 2 were obtained from Fig. 10. Isotherm

Table 2
Langmuir and Freundlich parameters for the adsorption of AB FGRL

Dye	Langmuir			Freundlich		
	q_m (mg g^{-1})	K (l g^{-1})	r^2	n	K_F (mg$^{1-1/n}$l$^{1/n}$g^{-1})	r^2
Astrazon Blue FGRL	312.5	0.15	0.916	2.05	5.24	0.987

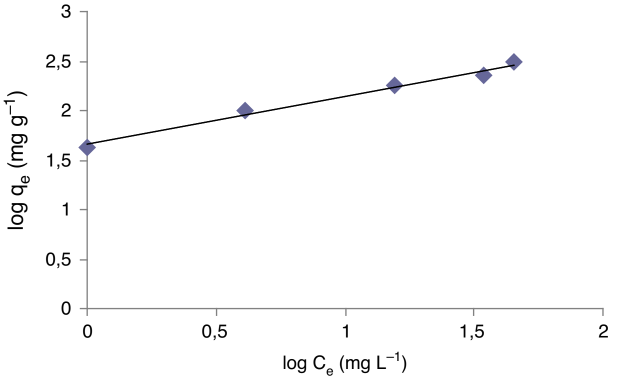

Fig. 10. Freundlich isotherm for adsorption of AB FGRL (293 K, 100 mg l^{-1}, solid–liquid: 0.1 g 200 ml^{-1}, pH = 7, particle size: 0.1–2.5 mm).

Table 1
Kinetics data calculated for adsorption of AB FGRL on sepiolite

Parameters			Kinetic models							
T (K)	C_0 (mg l^{-1})	pH	Pseudo-first-order				Pseudo-second-order			
			r^2	k_1 (min^{-1})	$q_{e\ experimental}$ (mg g^{-1})	$q_{e\ calculated}$ (mg g^{-1})	r^2	k_2 (g mg^{-1} min)	$q_{e\ experimental}$ (mg g^{-1})	$q_{e\ calculated}$ (mg g^{-1})
293	25	7	0.773	28.98	28.98	11.96	0.999	9.95×10^{-3}	28.98	30.03
293	50	7	0.785	88.285	88.285	59.84	0.999	1.84×10^{-3}	88.285	94.33
293	100	7	0.979	162.573	162.573	273.09	0.998	7.20×10^{-4}	162.573	178.57
293	150	7	0.922	243.429	243.429	273.09	0.998	6.25×10^{-4}	243.429	312.5
293	200	7	0.922	292.858	292.858	273.09	0.998	6.25×10^{-4}	292.858	312.5
283	100	7	0.959	162.573	162.573	72.36	0.999	1.00×10^{-3}	162.573	129.87
293	100	7	0.997	0.034	162.573	102.54	0.998	7.18×10^{-4}	162.573	178.57
303	100	7	0.952	0.035	162.573	54.66	0.998	8.62×10^{-4}	162.573	129.87

plot Freundlich isotherm model fits very well when the r^2 values are compared. One of the Freundlich constants (K_F) indicates the adsorption capacity of the adsorbent, while the other (n) is a measure of the deviation from linearity of the adsorption. If n value is equal to 1, the adsorption is linear; on the other hand if n is below 1, the adsorption process is chemical, and if n is above 1, adsorption is a favorable physical process. The value of n at equilibrium (2.05) suggests that physical adsorption is dominant with respect to chemical adsorption, which indicates weak adsorption bonds [53] and the presence of Van Der Waals forces.

4. Conclusions

Sepiolite (meerschaum), as an adsorbent, has a considerable potential for removing AB FGRL in adsorption systems because of its high surface area. Equilibrium adsorption was achieved in about 90 min. The adsorption is highly dependent on the concentration, pH and temperature of the solution. The pH value affects the surface charge of the adsorbent and the degree of ionization of adsorbate.

The kinetics of AB FGRL adsorption onto sepiolite (meerschaum) was examined by using the pseudo-first-order and pseudo-second-order kinetic models under different initial dye concentrations, temperatures and pHs. The pseudo-second-order proved to better predict the adsorption behavior agreeing with physisorption being rate-controlling because it is fundamentally based on the adsorption capacity.

The experimental data perfectly fitted with the Freundlich isotherm, showing that the surface of the sepiolite (meerschaum) particle is heterogeneous, non-specific and non-uniform in nature. It may be concluded that sepiolite (meerschaum) can be used for the selective sorption of textile dye effluents from wastewater. Sepiolite (meerschaum) can therefore be considered a low-cost, naturally abundant and locally available adsorbent for dye removal useable as an alternative to more expensive adsorbents such as activated carbon.

Acknowledgements

The authors wish to thank two anonymous reviewers for helpful suggestions that have improved the manuscript.

References

[1] Y. Ozdemir, M. Dogan and M. Alkan, Adsorption of cationic dyes from aqueous solutions by sepiolite, Microporous Mesoporous Mater., 96 (2006) 419–427.

[2] T. Robinson, B. Chandran and P. Nigam, Removal of dyes from a synthetic textile dye effluent by biosorption on apple pomace and wheat straw, Water Res., 36 (2002) 2824–2830.

[3] K.R. Ramakrishna and T. Viraraghavan, Dye removal using low cost adsorbents, Water Sci. Technol., 36 (1997) 189–196.

[4] P. Nigam, G. Armour, I.M. Banat, D. Singh and R. Marchant, Physical removal of textile dyes from effluents and solid-state fermentation of dye-adsorbed agricultural residues, Bioresour. Technol., 72 (2000) 219–226.

[5] M. Ugurlu, Adsorption of a textile dye onto activated sepiolite, Microporous Mesoporous Mater., 119 (2009) 276–283.

[6] C.R.S. Sílvia and A.R.B. Rui, Adsorption modelling of textile dyes by sepiolite, Appl. Clay Sci., 42 (2008) 137–145.

[7] A.S. Ozcan, B. Erdem and A. Ozcan, Adsorption of Acid Blue 193 from aqueous solutions onto BTMA-bentonite, Colloids Surf. A., 266 (2005) 73–81.

[8] Q.Y. Sun and L.Z. Yang, The adsorption of basic dyes from aqueous solution on modified peat-resin particle, Water Res., 37 (2003) 1535–1544.

[9] G.M. Walker and L.R. Weatherley, Kinetics of acid dye adsorption on GAC, Water Res., 33 (1999) 1895–1899.

[10] A. Ozcan, E.M. Oncu and A.S. Ozcan, Adsorption of Acid Blue 193 from aqueous solutions onto DEDMA-sepiolite, J. Hazard. Mater., 129 (2006) 244–252.

[11] S.F. Montanher, E.A. Oliveira and M.C. Rollemberg, Removal of metal ions from aqueous solutions by sorption onto rice bran, J. Hazard. Mater., 2–3 (2005) 207–211.

[12] F.L. Arbeloa, T.L. Arbeloa and I.L. Arbeloa, Spectroscopy of Rhodamine 6G adsorbed on sepiolite aqueous suspensions, J. Colloid Interf. Sci., 187 (1997) 105–112.

[13] G. Rytwo, D. Tropp and C. Serban, Adsorption of diquat, paraquat and methyl green on sepiolite: experimental results and model calculations, Appl. Clay Sci., 20 (2002) 273–282.

[14] B. Armagan, O. Ozdemir, M. Turan and M.S. Celik, Adsorption of negatively charged azo dyes onto surfactant-modified sepiolite, J. Environ. Eng., 129 (2003) 709–715.

[15] A.S. Ozcan, S. Tetik and A. Ozcan, Adsorption of acid dyes from aqueous solutions onto sepiolite, Sep. Sci. Technol., 39 (2004) 301–320.

[16] R.G. Harris, J.D. Wells and B.B. Johnson, Selective adsorption of dyes and other organic molecules to kaolinite and oxide surfaces, Colloid Surf. A., 180 (2001) 131–140.

[17] C.C. Wang, L.C. Juang, T.C. Hsu, C.K. Lee, C.F. Lee and F.C. Huang, Adsorption of basic dyes onto montmorillonite, J. Colloid Interf. Sci., 273 (2004) 80–86.

[18] M. Ogawa, R. Kawai and K. Kuroda, Adsorption and aggregation of a cationic cyanine dye on smectites, J. Phys. Chem., 100 (1996) 16218–16221.

[19] A.S. Ozcan, B. Erdem and A. Ozcan, Adsorption of Acid Blue 193 from aqueous solutions onto Na–bentonite and DTMA–bentonite, J. Colloid Interf. Sci., 280 (2004) 44–54.

[20] A.S. Ozcan and A. Ozcan, Adsorption of acid dyes from aqueous solutionsonto acid-activated bentonite, J. Colloid Interf. Sci., 276 (2004) 39–46.

[21] A. Tabak, E. Eren, B. Afsin and B. Caglar, Determination of adsorptive properties of a Turkish Sepiolite for removal of Reactive Blue 15 anionic dye from aqueous solutions, J. Hazard Mater., 161 (2009) 1087–1094.

[22] D. Gonzalez-Roman, M.D. Ruiz-Cruz, R. Pozas-Tormo, J.R. Ramos-Barrodo, C. Criado and L. Moreno-Real, Ionic conduction in sepiolite, Solid State Ionics, 61 (1993) 163–172.

[23] S. Akyuz, T. Akyuz and J.E.D. Davies, An FT-IR spectroscopic investigation of the adsorption of benzidine by sepiolite from Eskisehir (Turkey), J. Mol. Struct., 293 (1993) 279–282.

[24] M. Myriam, M. Suarez and J.M. Martin-Pozas, Structural textural modification of palygorskite and sepiolite under acid treatment, Clays Clay Miner., 3 (1998) 225–231.

[25] R. Giustetto, O. Wahyudi, I. Corazzari and F. Turci, Chemical stability and dehydration behavior of a sepiolite/indigo Maya Blue pigment, Appl. Clay Sci., 52 (2011) 41–50.

[26] S. Akyuz and T. Akyuz, Infrared spectrum investigations of adsorption and oxidation of N,N-dimethylaniline by sepiolite, loughlinite and diatomite, J. Inclusion Phenom., 5 (1987) 259–262.

[27] S. Yariv, Thermo-IR-spectroscopy analysis of the interactions between organic pollutants and clay minerals, Thermochim. Act., 274 (1996) 1–35.

[28] Y. Grillet, J.M. Cases, M. Francois, J. Rouquerol and J.E. Poirier, Modification of the porous structure and surface area of sepiolite under vacuumthermal treatment, Clays Clay Miner., 36 (1988) 233–242.

[29] M. Alkan, O. Demirbas and M. Dogan, Adsorption kinetics and thermodynamics of an anionic dye onto sepiolite, Microporous Mesoporous Mate., 101 (2007) 388–396.

[30] I. Rodriguez, M.P. Limpart and R. Cela, Solid-phase extraction of phenols, J. Chromatogr., 885 (2000) 291–304.

[31] M. Ugurlu, A. Gurses and M. Acıkyıldız, Comparison of textile dyeing effluent adsorption on commercial activated carbon and activated carbon prepared from olive stone by $ZnCl_2$ activation, Microporous Mesoporous Mate., 111 (2008) 228–235.

[32] B. Karagozoglu, M. Tasdemir, E. Demirbas and M. Kobya, The adsorption of basic dye (Astrazon Blue FGRL) from aqueous solutions onto sepiolite, fly ash and apricot shell activated carbon: kinetic and equilibrium studies, J. Hazard. Mater., 147 (2007) 297–306.

[33] K. Marungrueng and P. Pavasant, Removal of basic dye (Astrazon Blue FGRL) using macroalga *Caulerpa lentillifera*, J. Environ. Manage., 78 (2006) 268–274.

[34] S. Lagergren, Zur theorie der sogenannten adsorption gel oster stoffe, Kungliga Svenska Vetenskapsakademiens, Handlingar, 24 (1898) 1–39.

[35] A. Gurses, C. Dogar, M. Yalcin, M. Acikyildiz, R. Bayrak and S. Karaca, The adsorption kinetics of the cationic dye, methylene blue, onto clay, J. Hazard. Mater., 131 (2006) 217–228.

[36] M.I. El-Khaiary, Kinetics and mechanism of adsorption of methylene blue from aqueous solution by nitric-acid treated water-hyacinth, J. Hazard. Mater., 147 (2007) 28–36.

[37] M.S. El-Geundi, Homogeneous surface diffusion model for the adsorption of basic dyestaffs onto natural clay in batch adsorbers, Adsorpt. Sci. Technol., 8 (1991) 217–225.

[38] E. Rubin, P. Rodriguez, R. Herrero, J. Cremades, I. Barbara and M.E. Sastre de Vicente, Removal of Methylene Blue from aqueous solutions using as biosorbent *Sargassum muticum*: an invasive macroalga in Europe, J. Chem. Technol. Biotechnol., 80 (2005) 291–298.

[39] J.Q. Jiang, C. Cooper, and S. Ouki, Comparison of modified montmorillonite adsorbents. Part I. Preparation, characterization and phenol adsorption, Chemosphere, 47(7) (2002) 711–716.

[40] A. Alvarez, Sepiolite: properties and uses, in: A. Singer, E. Galan (Eds.), Developments in Sedimentology, Elsevier, Amsterdam, 1984, pp. 253–285.

[41] T. Kavas, E. Sabah and M.S. Celik, Structural properties of sepiolite-reinforced cement composite, Cem. Concr. Res., 34 (2004) 2135–2139.

[42] A. Ozcan and A.S. Ozcan, Adsorption of Acid Red 57 from aqueous solutions onto surfactant-modified sepiolite, J. Hazard. Mater., B125 (2005) 252–259.

[43] E. Eren, O. Cubuk, H. Ciftci, B. Eren and B. Caglar, Adsorption of basic dye from aqueous solutions by modified sepiolite: equilibrium, kinetics and thermodynamics study, Desalination, 252 (2010) 88–96.

[44] M. Yeniyol, Vein-like sepiolite occurrence as a replacement of magnesite in Konya, Turkey, Clays Clay Miner., 34 (1986) 353–356.

[45] W.T. Tsai, C.W. Lai and K.J. Hsien, Adsorption kinetics of herbicide paraquat from aqueous solution onto activated bleaching earth, Chemosphere, 55 (2004) 829–837.

[46] D. Singh, Effect of different factors on the adsorption of phosphamidon on two different types of Indian soil, Adsorpt. Sci. Technol., 16 (1998) 583–594.

[47] M. Dogan, Y. Ozdemir and M. Alkan, Adsorption kinetics and mechanism of cationic methyl violet and methylene blue dyes onto sepiolite, Dyes Pigm., 75 (2007) 701–713.

[48] M. Alkan, O. Demirbas and M. Dogan, Electrokinetic properties of sepiolite suspensions in different electrolyte media, J. Colloid Interf. Sci., 281 (2005) 240–248.

[49] M. Dogan and M. Alkan, Adsorption kinetics of methyl violet onto perlite, Chemosphere, 50 (2003) 517–528.

[50] M. Doğan, M. Alkan, A. Turkyılmaz, and Y. Ozdemir, Kinetics and mechanism of removal of methylene blue by adsorption onto perlite, J. Hazard. Mater., B109 (2004) 141–149.

[51] I.D. Mall and S.N. Upadhyay, Treatment of methyl violet bearing wastewater from paper mill effluent using low cost adsorbents, Indian Pulp Paper Tech. Assoc., 51 (1995) 51.

[52] I. D. Mall, V.C. Srivastava and N.K. Agarwal, Removal of Orange-G and Methyl Violet dyes by adsorption onto bagasse fly ash, kinetic study and equilibrium isotherm analyses, Dyes Pigm., 69 (2006) 210–223.

[53] S. Dikmen, G. Yilmaz, E. Yorukogullari and E. Korkmaz, Zeta potential study of natural- and acid-activated sepiolites in electrolyte solutions, Can. J. Chem. Eng., 9999 (2011) 1–8.